BNL-224703-2023-JAAM

Evaluation of electron lifetime for Te inclusions free CdZnTe

K. Kim, A. Bolotnikov

To be published in "Nuclear Instruments and Methods in Physics Research Section A: Accelerators, Spectrometers, Detectors and Associated Equipment"

October 2023

Instrumentation Division

Brookhaven National Laboratory

U.S. Department of Energy

USDOE Office of Science (SC), Nuclear Physics (NP) (SC-26)

DISCLAIMER

Evaluation of electron lifetime for Te inclusions free CdZnTe

Kihyun Kim [a], Aleksey E. Bolotnikov [b] , Ralph B. James [c]

[a] School of Health and Environmental Science, Korea University, Seoul, 02841, Korea
[b] Brookhaven National Laboratory, Upton, 11973, NY, USA
[c] Savannah River National Laboratory, Aiken, 29808, SC, USA

Abstract

Te secondary phase defects are known as major obstacle for improving charge carriers transport properties of CdTe compounds material. The enhanced detector performance was reported for Te inclusions free CZT detector implemented through two-step annealing (i.e., first in Cd and second in Te). We applied the time-of-flight (TOF) technique to measure the electron lifetime in as-grown and two-step annealed CZT material. TOF has several advantages over Hecht equation fitting such as independence of the electric field distribution, direct measurement of carrier lifetime, and high accuracy for high mobility-lifetime product CZT material. The detector performance improved drastically for the two-step annealed CZT detector except which containing inordinate number and size of prismatic punching defects. The average electron lifetime increased more than 10 times after successful two-step annealing.

Keywords: CdZnTe, time-of-flight, mobility-lifetime product, Te inclusions free, two-step annealing

1. Introduction

CdZnTe (CZT) is the leading material for large-volume room temperature X- and gamma-ray detectors. High performance radiation detectors require good electrical properties such as high carrier mobility and long carrier lifetime. Te secondary phase defects in CdTe compounds refer to the presence of Te-rich secondary phase within the crystal structure, like Te inclusions and Te precipitates. Te inclusions which bigger than 5 μm are most critical effect on the charge trapping [1] and internal electric field distribution [2]. Te inclusions are generated during the CZT growth process at the unstable liquid-solid interface by capturing of the Te-rich melts. Te inclusions can be removed easily by Cd overpressure annealing between 600 and 800 ℃ but the resistivity of CZT samples drop down from 10 10 Ω·cm to 10 3 Ω·cm. There is several research which report successful Te inclusions removal while keeping its resistivity through two-step annealing (i.e. first annealing under Cd vapor and second annealing in Te ambient environment) [3, 4] or Te vapour annealing [5, 6].

The detrimental effect of Te secondary phase defect can be overcome applying high bias voltage for 2-3 mm thick planar CZT detectors. However, cumulativeness of small-sized Te inclusions in large volume yield critical effect on the non-uniform internal electric fields and severe electron clouds trapping.

The principle of time-of-flight (TOF) technique is measuring the dependence of the collected charge versus the drift time across a long sample. TOF has several advantages over Hecht equation fitting. It is independent on the electric field distribution in sample and offer a direct measurement of carrier lifetime. Also, it is very sensitive technique

for measuring carrier lifetime in high carrier lifetime and mobility products (> 10^{-2} cm^2 /V) materials [7].

Te inclusions free CZT exhibited improved carrier lifetime-mobility products and enhanced detector performance in the gamma-ray spectroscopy. It might be caused by the minimized carrier trapping and scattering due to the Te secondary phase defect [8]. In this paper, the effects of two-step annealing on the electron lifetime was quantitatively analyzed by TOF technique.

2. Experiment

2-inch $Cd_{0.9}Zn_{0.1}Te$ ingot was grown by Bridgman method from a mixed melt of CdTe (6N), ZnTe (6N), Te (7N), and In (7N). The typical growth rate and an interface temperature gradient were 3 mm/h and 10–15 ℃/cm, respectively. The as-grown CdZnTe ingots were sliced parallel to their growth direction. Four pairs of 6 × 6 × 12 mm^3 single crystals are harvested from adjacent region of CZT wafers and finalized via mechanical and chemical polishing. In each pair of CZT samples, one sample was used for annealing and the other sample was used for control sample. Before the electrode formation by electro-less method using AuCl 3 solution, CZT samples are dipped into 0.05 % of Br-MeOH solution for 30 min.. The resistivity of CdZnTe was measured by two-probe current-voltage measurements using Keithley 237. The electrical resistivity of as-grown CZT is (3-5) × 10^{10} Ω·cm depending on their position in the ingot.

For a two-step annealing, the quartz tubing of CZT/source which sealed in a vacuum of 10^{-6} torr was placed in the two-zone furnace. For the Cd overpressure annealing, the quartz tubing containing CZT and Cd source kept at 450 ℃/600 ℃ for in-diffusion of Cd then raised to 600 ℃/600 ℃ slowly to prevent drastic chemical reaction between elemental Cd and Te inclusions. In case of the Te ambient annealing, the quartz tube containing Cd annealed CZT and Te source kept at 500 ℃/520 ℃. The annealing time varied depending on the sample thickness.

The existence or nonexistence of prismatic punching defect in two-step annealed samples were revealed by Nakagawa etchant. Drift time of Frisch grid CZT detectors was measured by TOF system. Details on the TOF system can be found in reference [7]. Metallic Frisch-grid in CZT detector was set as common grounding point while taking anode and cathode signal simultaneously. The gain of CR-110(Cremat Inc.) preamplifier is 1.4 V/pC thus highest signal output amplitude of preamplifier for 662 keV is about 32.9 meV considering full electron collection.

For the pulse height measurements at room temperature, the Frisch-grid CZT detector was installed in a detector holder, and the cathode side of the detector was irradiated using a radioisotope. The signals from the positively biased anode were measured by using a capacitively coupled CR-110(Cremat Inc.) preamplifier. The data acquisition system included a spectroscopic shaping amplifier and a multi-channel analyzer (MCA).

3. Results and Discussion

Figure 1 shows characteristics of current-voltage in as-grown and twostep annealed CZT detectors. The electrical resistivity of two-step annealed CZT is similar or slightly higher than that of as-grown CZT. Quasi-ohmic contact behavior might come from stoichiometric CZT surface/gold contact. Low concentration of Br-solution etching lessens selective etching of metallic element.

The electronic signal generated by Cs-137 source were captured from the cathode and anode with a digital oscilloscope. At that time, high threshold trigger was set on the cathode signal to select the photo-peak events near the cathode. The longest anode signals with amplitudes more than 30 meV were captured to ensure that the captured waveforms represent the photoabsorption events when the electron clouds drift nearly a full length of the detector. Drift time was set an interval time between the sharp rising edge of the cathode signal and the tip of the anode signal.

Figure 2 and 3 represents typical waveforms of anode and cathode signals measured at pre-amplifier stage for as-grown and two-step annealed CZT, respectively. As an applied bias increase, the anode signal amplitude increased up to its maximum value due to complete charge collection and the electron drift time diminished in both CZT detectors. The clear signal can be obtained above 600 V for as-grown CZT detector and above 100 V for two-step annealed CZT detector. However, one of two-step annealed Frisch-grid CZT detector exhibited longer drift time than other two-step annealed Frisch-grid CZT detectors.

The electron clouds which generated near the surface of a planar detector will drift across the detector towards the anode. The collected charge is proportional to the amplitude of the signals measured from the anode [9].

$$Q = Q_0 \exp(-t/\tau) \quad \ldots\ldots (1)$$
$$\ln(Q/Q0) = -t/\tau \quad \ldots\ldots (2)$$

where Q is collected charge, Q_0 is fully collected charge, and τ is carrier lifetime. The electron lifetime was extracted from the fitting of the dependence of the amplitude versus collected charge measured at different biases.

The electron lifetime is in the range of 2 ~ 3 μs for as-grown CZT and 13 ~ 14 μs for two-step annealed CZT shown in Fig. 4. Te inclusions are known as a carrier trapping center which deteriorating the performance of CZT detector. There is well known correlation between the energy resolution and the mobility-lifetime product of CZT detector and the size and concentration of Te inclusions [10]. The enhancement of the carrier lifetime in two-step annealed CZT is matter of fact. However, all the two-step annealed CZT does not showed drastic improvement in the electron lifetime as depicted in Fig. 4(b).

For the detectors, heavily decorated prismatic punching defects were found in surface etching with HF-based solutions shown in Fig. 5. In previous research, star-shaped prismatic punching defects were generated during the Cd overpressure annealing by the acute reaction of Te inclusions and Cd vapour [11, 12] and showed prismatic punching defect is a kinds of dislocations defects [13]. The size of prismatic punching defects is ranging from tens to few hundreds micrometers. Also, the density of these features is in the range of $2 \times 10^2 \sim 1 \times 10^3$ per cm^3 [13]. Dislocation generates a

trap level within the band gap at 0.2 eV above valence band [14]. Thus, CZT detector heavily decorated with prismatic punching defects did not show drastic enhancement in the detector performance due to the dislocation induced carrier trapping.

From IR transmission microscopy analysis of the control sample, we did not found big-sized (100 μm) Te inclusions but many aggregate of small-sized Te inclusions. It means that the distribution of Te inclusions is also important factor in the generation of prismatic punching defects in Cd overpressure annealing.

Figure 6 show the typical pulse height spectra of Cs-137 taken by as-grown and two-step annealed Frisch-grid CZT detector. The energy resolution of as-grown and two-step annealed CZT detector for 662 keV is about 6% and 2% without any correction. In addition, peak to Compton (PC) and peak to valley (PV) ratio is notably improved after two-step annealing. For the application of high energy detection, Te inclusions should be removed through the optimization of CZT crystal growth process or post-growth processing.

4. Summary

The electron lifetime of as-grown and two-step annealed CZT was evaluated by TOF experiment. The electron lifetime in as-grown and two-step annealed CZT sample is 2 ~ 3 μs and 13 ~ 14 μs, respectively. The information of Te inclusion on size as well as its distribution is important factor to eliminate Te inclusions by two-step annealing without the generation of prismatic punching defects. The aggregate of 10 ~ 30 μm Te inclusions behave similar to few hundreds μ m sized Te inclusions in Cd overpressure annealing process. Post-growth annealing processes are one of the key techniques to obtain high electron carrier-lifetime products (> 10^{-2} cm^2/V) CZT material and essential for high energy application.

Acknowledgement

This work was supported by the National Research Foundation of Korea (NRF) grant funded by Korea government (MSIT) (No. 2021R1A2C1012161).

References

[1] A. Bolotnikov, N. Abdul-Jabbar, O. Babalola, G. Camarda, Y. Cui, A. Hossain, E. Jackson, H. Jackson, J. James, K. Kohman, et al., Effects of Te inclusions on the performance of CdZnTe radiation detectors, IEEE Transactions on nuclear science 55 (5) (2008) 2757–2764.

[2] A. Wardak, M. Witkowska-Baran, M. Szot, D. Kochanowska, B. S. Witkowski, A. Avdonin, A. Mycielski, Electric field distribution around cadmium and tellurium inclusions within CdTe-based compounds, Journal of Crystal Growth 533 (2020) 125486.

[3] K. Kim, S. Hwang, H. Yu, Y. Choi, Y. Yoon, A. E. Bolotnikov, R. B. James, Two-step annealing to remove Te secondary-phase defects in CdZnTe while preserving the high electrical resistivity, IEEE Transactions on Nuclear Science 65 (8) (2018) 2333–2337.

[4] M. Bugar, E. Belas, R. Grill, J. Prochazka, S. ˇ Uxa, P. Hlidek, J. Franc, R. Fesh, P. Hoschl, Inclusions elimination and resistivity restoration of CdTe:Cl crystals by two-step annealing, IEEE Transactions on nuclear science 58 (4) (2011) 1942–1948.

[5] G. Piacentini, N. Zambelli, G. Benassi, D. Calestani, M. Pavesi, A. Zappettini, Two-step thermal process in tellurium vapor for tellurium inclusion annealing in high resistivity CdZnTe crystals, Journal of Crystal Growth 415 (2015) 15–19.

[6] J. Franc, L. ˇ Sediv`y, E. Belas, M. Bugar, J. Z´azvorka, J. Pek´arek, S. ˇ Uxa, P. H¨oschl, R. Fesh, Melt growth and post-grown annealing of semiinsulating (CdZn) te by vertical gradient freeze method, Crystal Research and Technology 48 (4) (2013) 214–220.

[7] A. Bolotnikov, G. S. Camarda, E. Chen, R. Gul, V. Dedic, G. De Geronimo, J. Fried, A. Hossain, J. MacKenzie, L. Ocampo, et al., Use of the drift-time method to measure the electron lifetime in long-drift-length CdZnTe detectors, Journal of Applied Physics 120 (10) (2016) 104507.

[8] E. Kim, Y. Kim, A. Bolotnikov, R. James, K. Kim, Detector performance and defect densities in CdZnTe after two-step annealing, Nuclear Instruments and Methods in Physics Research Section A: Accelerators, Spectrometers, Detectors and Associated Equipment 923 (2019) 51–54.

[9] A. Bolotnikov, G. Camarda, G. Carini, M. Fiederle, L. Li, G. Wright, R. James, Performance studies of CdZnTe detector by using a pulse shape analysis, in: Hard X-Ray and Gamma-Ray Detector Physics VII, Vol. 5922, International Society for Optics and Photonics, 2005 p. 59220K.

[10] A. E. Bolotnikov, N. Abdul-Jabber, S. Babalola, G. S. Camarda, Y. Cui, A. Hossain, E. Jackson, H. Jackson, J. James, K. T. Kohman, A. Luryi, R. B. James, Effects of Te inclusions on the performance of CdZnTe radiation detectors, in: 2007 IEEE Nuclear Science Symposium Conference Record, 2007.

[11] K. Kim, A. Bolotnikov, G. Camarda, J. Franc, P. Fochuk, R. James, Prismatic punching defects in CdTe compounds, Journal of crystal growth 390 (2014) 1–4.

[12] G. Yang, A. Bolotnikov, P. Fochuk, Y. Cui, G. Camarda, A. Hossain, K. Kim, B. Raghothamachar, U. Roy, R. James, ‘Star-like’defects in Cdannealed CdZnTe crystals—an experimental study of their origin and formation mechanism, Crystal Research and Technology 48 (4) (2013) 221–226.

[13] A. Hossain, A. Bolotnikov, G. Camarda, Y. Cui, G. Yang, K. Kim, R. Gul, L. Xu, R. James, Extended defects in CdZnTe crystals: Effects on device performance, Journal of Crystal Growth 312 (11) (2010) 17951799.

[14] R. Soundararajan, K. G. Lynn, Effects of excess tellurium and growth parameters on the band gap defect levels in $Cd_xZn_{1-x}Te$, Journal of Applied Physics 112 (7) (2012) 073111.

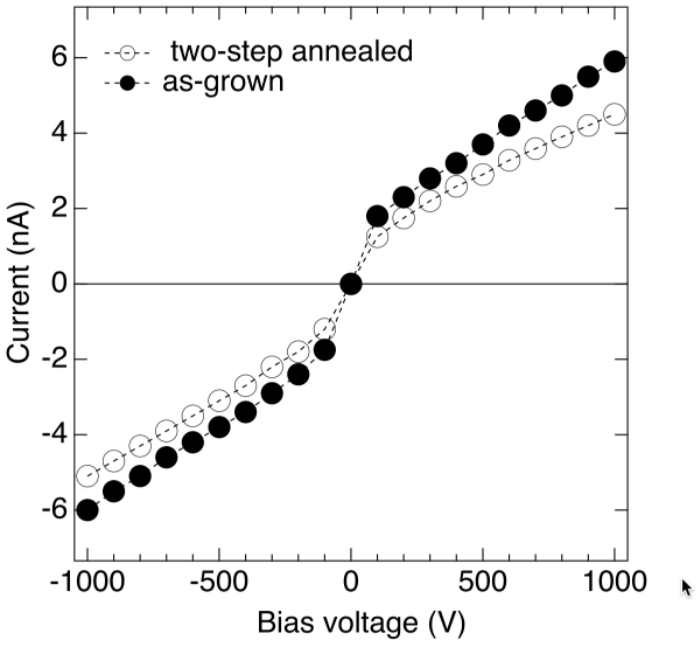

Figure 1: Characteristic current-voltage curves of as-grown and two-step annealed CZT detectors. Emersion of CZT samples at low concentration of Br-MeOH prior to electrode formation makes quasi-Ohmic shape.

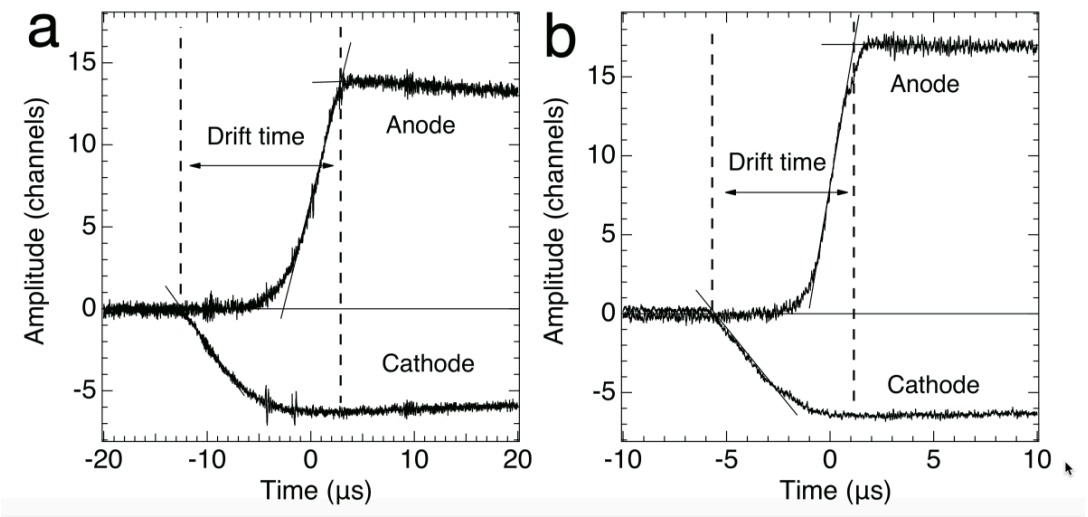

Figure 2: Representative waveforms of anode and cathode signals measured at a) 800 V and b) 1300 V for 6×6×12 mm^3 Frisch-grid CZT detector which fabricated with as-grown CZT. Other three as-grown CZT detectors also showed similar amplitude and drift time. The cathode signal is used to evaluate the starting time of an electron cloud as it drifts towards the anode. Drift time is 15.2 μs for 800 V and 6.9 μs for 1300 V.

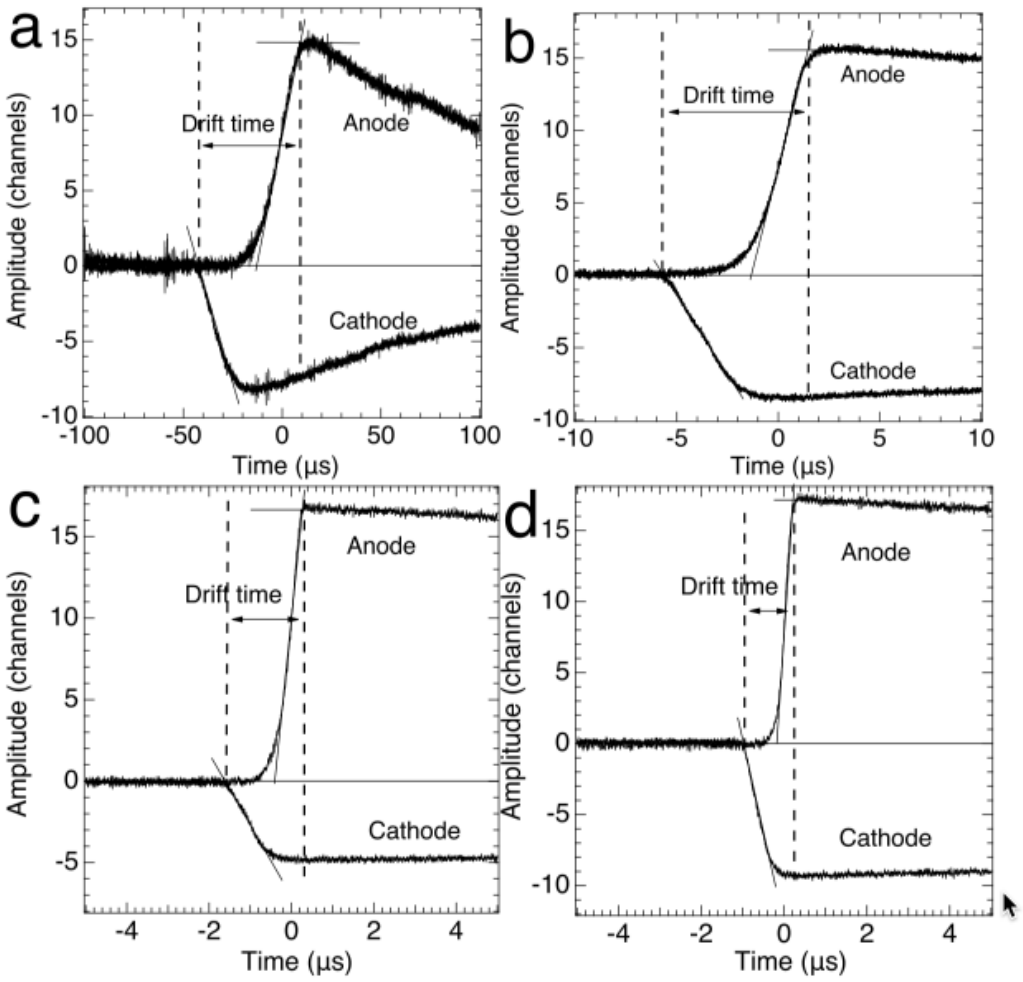

Figure 3: Representative waveforms of anode and cathode signals measured at a) 100 V, b) 400 V, c) 800 V, and d) 1200 V for 6×6×12 mm^3 Frisch-grid CZT detector which fabricated with two-step annealed CZT. The cathode signal is used to evaluate the starting time of an electron cloud as it drifts towards the anode.

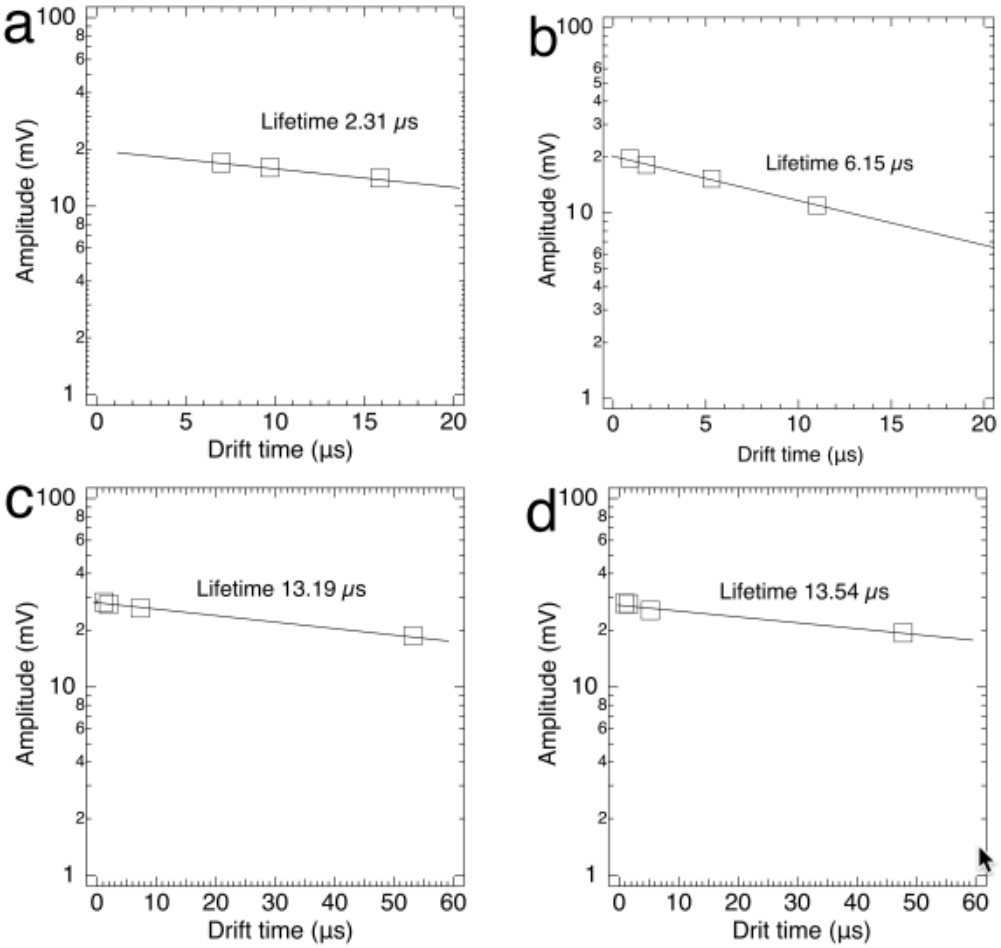

Figure 4: Representative waveforms of anode and cathode signals measured at different bias for 6×6×12 mm^3 Frisch-grid CZT detector with two-step annealed CZT. The cathode signal is used to evaluate the starting time of an electron cloud as it drifts towards the anode.

Figure 5: Prismatic punching defects appeared in an annealed CZT after HF-based solutions etching. The size of photograph is 6 × 6 cm^2. The density of these features is in the range of $2 \times 10^2 \sim 1 \times 10^3$ cm^{-3} considering isotropic and uniform distribution.

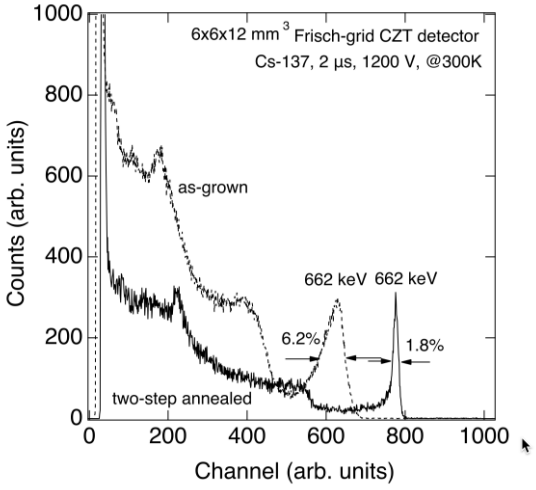

Figure 6: Pulse height spectra of Cs-137 taken with as-grown and two-step annealed Frisch-grid CZT detectors at 1200 V.